B.Sc. (Hons) Physics Project

Thesis

Samuel Moore
School of Physics, University of Western Australia
April 2012

Characterisation of Nanostructured Thin Films

Keywords: surface plasmons, nanostructures, spectroscopy, metallic-blacks
Supervisers: W/Prof. James Williams (UWA), Prof. Sergey Samarin (UWA)

Acknowledgements

I am extremely grateful for the support offered to me by many individuals during this project.

1 Introduction

2 Overview of Theory

Summarise the literature, refer to past research etc

2.1 Electron Spectra of Solids and Surface

In this section, we will first introduce the basic concepts needed to describe the electron spectra of solids. A short description of methods for calculating the electron spectra will be given, and the results shown by these calculations. We will then discuss the electron spectra for the near surface region of solids, compared to the "bulk" spectra far from the surface.

2.1.1 Description of Matter in the Solid State

In the simplest models, a solid is represented by an infinite crystalline lattice; a geometrically repeated arrangement of some basis group of atoms. The nuclei of atoms are assumed to remain in fixed positions.

The potential seen by an electron in the lattice is periodic. For a single nuclei, the potential seen by an electron is

2.1.2 Calculation of Electron Spectra

2.1.3 The Near-Surface Region

In the preceeding sections, solids were assumed to have infinite spatial extent. In practice, any real solid occupies a finite volume in space. Any interactions between a solid and its environment take place at the surface of the solid. As the volume of the solid is decreased, the role of the surface region in determining the behaviour of the solid in its environment is increased.

2.2 Plasmonics

2.3 Metallic-Black Thin Films

3 Experimental Techniques

3.1 Secondary Electron Spectroscopy

Secondary Electron Spectroscopy encompasses a large group of techniques used for studying the electron spectra of surfaces and solids. In these methods a beam of primary electrons is directed at a surface. The interactions between primary electrons and the surface give rise to an energy distribution of electrons elastically and inelastically scattered from the surface. Analysis of the distribution of the scattered "secondary" electrons gives information about the electron energy spectrum of the target surface.

Figure 1: Simple model of the secondary electron distribution

Figure **??** shows the general shape of the secondary electron distribution for a primary electron energy of E_p. The narrow peak centred at $E = E_p$ is due to elastically scattered electrons; the width of this peak is determined by the distribution of primary electron energies, as well as the resolution of the detector. The broad peak in the low energy part of the spectrum is due to inelastically scattered electrons.

Real secondary electron distributions also show fine structure imposed on the inelastic part of the spectrum. This fine structure is characteristic of the target surface. Near to the elastic peak, fine structure is caused by energy loss to interband transitions and plasma vibration excitation. The central part of the distribution contains fine structure due to Auger electron emission, and energy losses due to excitation of inner electrons. Fine structure at low energies is due to the structure of empty states of the solid.

3.1.1 Methods of Secondary Electron Spectroscopy

Techniques of Secondary Electron Spectroscopy can be divided into two classes. Energy-resolved methods are based upon observation of the secondary electron distribution at a fixed primary electron energy. These methods aim to examine specific secondary emission processes which occur within a selected energy interval. In contrast to Energy-resolved methods, Total Current (or Yield) methods measure the total current of secondary electrons as a function of primary electron energy.

The focus of this project has been on low energy Total Current spectroscopy. While Total Current methods provide less detailed information about secondary emission processes within a solid, they are useful for

characterisation of the electron structure. Total Current methods are also simpler to realise experimentally, as they do not require energy analysers, and current measurement may be performed external to the vacuum chamber.

3.2 Total Current Secondary Electron Spectroscopy

Figure **??** shows a simplified schematic for the Total Current Spectroscopy experiments conducted during this study. Electrons are emitted from a cathode held at negative potential relative to the target. The electron beam is focused and accelerated onto the target by the electric field of an electron gun. A detector is used to measure the total current passing through the target.

Figure **??** is a block diagram of the experimental setup including measurement and control systems external to the vacuum chamber.

3.2.1 Electron Optics

The electron gun used for this experiment was repurposed from an old Cathode-Ray Oscilloscope (CRO). Figure **??** shows a simplified diagram of the electron gun, whilst Figure **??** shows a photograph of the gun.

The full circuit diagram for the electron gun control circuit is shown in Appendix A.

3.2.2 Automatic Data Acquisition

In order to collect data on the large number of planned samples for the study, some form of automation was required. The automated system needed to be able to incrementally set the initial energy by controlling a power supply, and record the total current measured by an ammeter.

The available power supplies at CAMSP featured analogue inputs for external control. This meant that a Digital to Analogue Convertor (DAC) card was needed to interface between the control computer and the power supply. In addition, the available instruments for current measurement at CAMSP produced analogue outputs. As a result, Analogue to Digital Convertors (ADCs) would be required to automate the recording of total current.

Although an external DAC/ADC box was already available for these purposes, initial tests showed that the ADCs on the box did not function. The decision was made to design and construct a custom DAC/ADC box, rather than wait up to two months for a commercial box to arrive. The design of the custom DAC/ADC box is discussed in detail in Appendix B, and the software written for the on-board microprocessor and the controlling computer are presented in Appendix D.

3.3 Ellipsometry and Transmission Spectroscopy

4 Experimental Results and Discussion

4.1 TCS Measurements

4.2 Ellipsometric Measurements

5 Achievements

Appendix A - Electron Gun Control and Current Measurement Circuit

Figure **??** shows the complete electron gun control circuit. The circuit was designed and constructed as part of this project. The design is based upon examples found in [**?**] and [**?**].

s

Appendix B - DAC/ADC Box - Hardware

Overview

In order to automate TCS experiments, both Digital to Analogue and Analogue to Digital Convertors were required (DAC and ADC). To provide these, a custom DAC/ADC Box was designed and constructed. The box can be controlled by any conventional computer with available RS-232 serial communication (COM) ports. Most modern computers no longer feature COM ports; a commercially available convertor can be used to interface between the box's RS-232 output and a standard Universal Serial Bus (USB) port.

The key components of the DAC/ADC box hardware include:

- Microprocessor (AVR Butterfly ATMega169)
- Four Analogue to Digital Converter (ADC) inputs
- Single Digital to Analogue Converter (DAC) output (Microchip MCP4922)
- Analogue electronics for amplification at ADC inputs and DAC outputs
- Seperate power supply circuitry for Digital and Analogue electronics
- RS-232 communications for control by a conventional PC or laptop

Microprocessor

The DAC/ADC box has been based upon Atmel's AVR Butterfly; an inexpensive and simple demonstration board for the ATMega169 16 Bit microprocessor. The features of the AVR Butterfly include easily accessible ports for Analogue to Digital Convertor (ADC) inputs and digital input/output, an onboard Universal

Asynchronous Reciever/Transmitter (USART) for RS-232 serial communications, and a 6 character Liquid Crystal Display (LCD). The AVR Butterfly can be programmed using a conventional computer over the USART using a RS-232 COM port. For modern computers (which do not usually posess COM ports), a RS-232 to USB converter may be used.

Figure 1 is a labelled photograph of the AVR Butterfly showing the use of the available ports for this project.

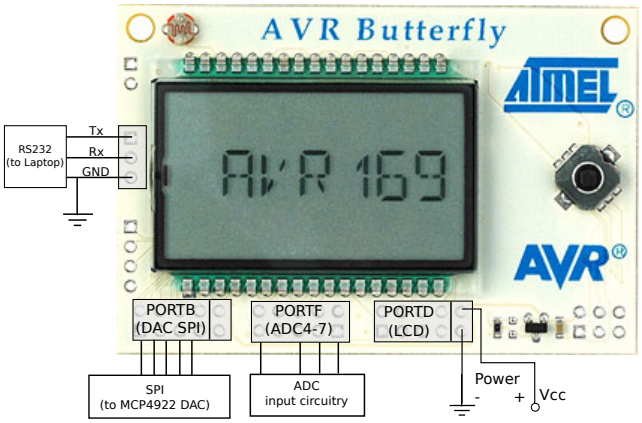

Figure 2: AVR Butterfly

Unless otherwise stated, all voltage differences are specified relative to the power supply ground of the AVR Butterfly.

ADC Inputs

The AVR Butterfly offers easy access to four of the ATMega169's ADCs through PORTF. Each ADC is capable of measuring voltages of $0 < V_{\text{adc}} < V_{cc}$ with 10 Bit resolution. For measuring voltages outside this range, some circuitry is required between the input voltage and the ADC input. In addition, it is desirable to provide the ADC with some form of input protection against accidental overloading. Figure 2 shows the input circuit which was used for three of the four available ADCs.

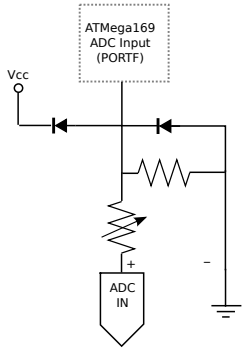

Figure 3: ADC4,6,7 Input

For making voltage measurements above V_{cc}, a voltage divider allows reduction of the voltage at the ADC. By constructing the voltage divider using a variable resistor, the range of measurable inputs could be manually adjusted.

The diodes shown in Figure 2 ensure that the ADC is protected from accidental exposure to voltages outside the acceptable range. In normal operation both diodes are off. If V_{adc} were to become greater than the reference point V_{cc}, current would flow between the ADC input and the reference point, acting to reduce V_{adc} until it reached V_{cc}. Similarly, if V_{adc} fell below ground, current would flow from ground to the ADC input, acting to increase V_{adc} until it reached ground.

The voltage at the ADC input can be related to the input of the voltage divider using Kirchoff's Voltage Law and Ohm's Law:

$$V_{\text{adc}} = \frac{R_1}{R_1 + R_2} V_{\text{in}}$$

Where V_{in} is the voltage at the input of the circuit, R_1 is a fixed resistor, and R_2 is variable resistor.

V_{in} can be therefore be determined from the registered ADC counts by:

$$V_{\text{in}} = \left(\frac{\text{ADC counts}}{2^{10}} \right) \times \frac{R_1 + R_2}{R_1} V_{cc}$$

Differential ADC Input

During the testing of the TCS experimental apparatus, it became desirable to measure the emission current of the electron gun. The electrometer used for this current measurement was capable of producing an analogue output in the range of $0 - 1V$. However, the negative terminal of this output was not at ground potential, but rather at the same terminal as the negative input terminal. Directly connecting the electrometer output to one of the ADC inputs discussed above would create a short circuit between the initial energy power supply, and ground (refer to Figures **??** and **??**). Therefore, it was decided to add a differential stage before the input of one of the ADCs.

Figure 3 shows the modification made to the input for ADC5 on the AVR Butterfly. The original voltage divider and input protection discussed above are still present. The modifications include the addition of an instrumentation amplifier, and low pass filters.

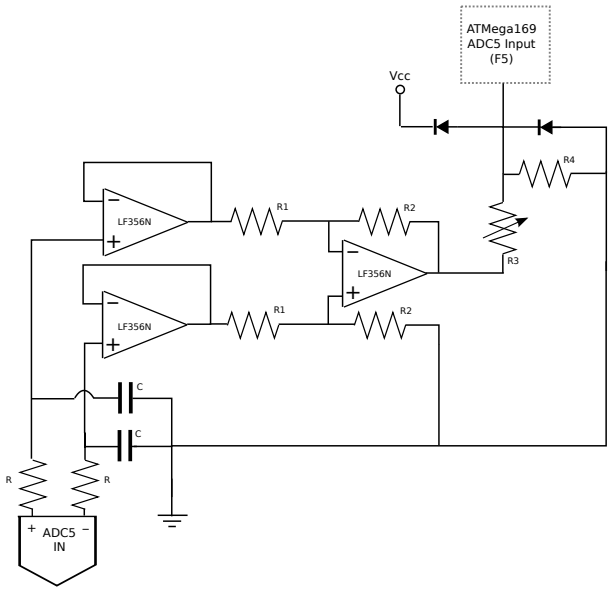

Figure 4: Differential Input stage for ADC5

asdfa The instrumentation amplifier consists of two stages of operational amplifiers (op-amps); input buffers, and a difference amplifier. The difference amplifier can be shown using the ideal op-amp model to produce an output voltage proportional to the difference between its inputs:

$$V_{out} = \frac{R_2}{R_1}(V_2 - V_1)$$

The two op-amps at the inputs to the differential amplifier are unity gain buffers. Although the outputs of the op amps are equal to their inputs, current is prevented from flowing from the circuit under measurement, and is instead drawn from the op amp power supply.

In principle, two ADC channels could be used to record the positive and negative outputs of the electrometer seperately, with differencing done in software. However this would require modification to the output cable of the electrometer, which may prove inconvenient for future uses.It was decided that the modification of the cable and added complexity of the software required would be more time consuming than differencing the two inputs using the hardware methods described above.

The low pass filters were added to the inputs of ADC5 after it was found that an unacceptable level of AC noise was being output by the electrometer. The level of noise was too high to be filtered in software, for reasons that will be discussed in Appendix D.

Temperature Measurement

The AVR Butterfly features an onboard thermistor connected to ADC0. Reading ADC0 and applying the formula given in the AVR Butterfly User's Guide [] results in a temperature measurement. This was useful in establishing a link between the changing chamber pressure and the temperature of the laboratory (see Appendix C).

Power Supplies

Due to the presence of both analogue and digital electronics in the DAC/ADC box, three seperate supply voltages were required:

1. Digital logic in the range $3 \rightarrow 4.5$V
2. Positive op-amp supply in the range $10 \rightarrow 15$V
3. Negative op-amp supply in the range $-10 \rightarrow -15$V

Circuitry was designed which allowed two seperate single pole power supplies to be used for Digital logic and the op-amps. A dual 0-30V DC power supply has been used for both digital and analogue circuitry.

Logic Power Supply

The AVR Butterfly runs off $3V < V_{cc} < 4.5V$ DC. Since V_{cc} was also used as the reference voltage for the ADCs and DAC output, it was desirable that V_{cc} be kept constant, despite the absolute level of the power supply. A $3.3V$ voltage regulator has been used for this purpose. The capacitor further smooths the output by shorting high frequency fluctuations to ground.

When the DAC/ADC box was first constructed V_{cc} was supplied by three $1.5V$ batteries. However, due to higher than expected power usage, and the unreliability of the voltage regulator as the input voltage fell below $4V$, inputs for an external power supply were later added.

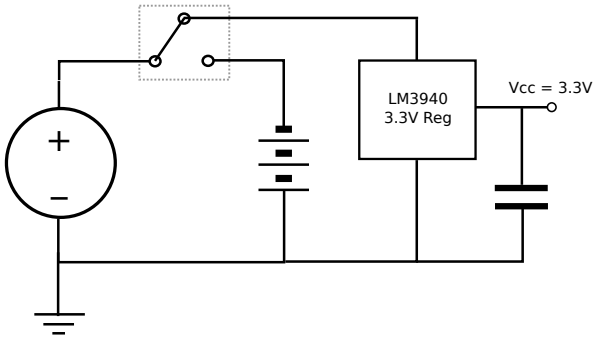

Figure 5: Logic Power Supply

Op-amp Power Supply

The DAC/ADC box circuitry involves several operational amplifiers (LF356), which require dual $\pm 10 - 15V$ supplies. As there were no dual $\pm$ power supplies available, a single $30V$ power supply was used, with the circuit shown in figure **??** used to produce $\pm 15V$ relative to ground.

The buffer amplifier ensures that negligable current can flow from the power supply into the logic and ADC circuits, whilst the capacitor removes high frequency fluctuations of the power supply relative to ground.

DAC Output

A commercial DAC board was used to produce the DAC output. The Microchip MCP4922 ET-Mini DAC is controlled by the AVR Butterfly using Motorola's Serial Peripheral Interface (SPI) Bus. The software used to implement SPI between the MCP4922 and the AVR Butterfly is discussed in Appendix D.

The ET-Mini DAC can only be powered off $3V$ to $5V$. Using $V_{cc} = 3.3V$ means that the DAC output cannot exceed $V_{cc} = 3.3V$. For TCS, energies of up to $15eV$ are required, so amplification of the DAC output was clearly necessary. A simple non-inverting amplifier with a manually adjustable gain was used to amplify the DAC output by a factor of three. This output was then used to control a laboratory power supply to produce the full range of initial energies.

RS-232 Communications

The AVR Butterfly features an onboard USART, which can be used both for programming and communication with the ATMega169 processor. The RS-232 communications requires only three wires; Recieve (RX), Transmit (TX) and a common ground.

The requirement that the AVR Butterfly share a common ground with the controlling computer lead to increased noise through ground loops. This is discussed in more detail in Appendix D.

Although the RS-232 is relatively simple to implement, which makes it ideal for non-proprietry microprocessor applications, most modern computers no longer feature RS-232 COM ports. Although a computer with COM ports was available at CAMSP, due to the extreme unreliability of this computer, it was quickly replaced

with a laptop that did not possess COM ports, and a commercial RS-232 to USB converter was used to interface with the laptop.

Appendix C - Pressure Monitoring

The pressure in the chamber was monitored by a ion gauge at low pressure (below 10^{-3} mbar), and a pirani gauge at high pressure. The gauge included a flurescent Liquid Crystal Display (LCD). In order to automate monitoring of pressure, a USB webcam was placed in front of the gauge LCD. Software was written using the Python Imaging Library (PIL) to convert the image produced by the webcam into a pressure reading. In this way, the pressure could be recorded as a function of time, independent from other measurements performed using the ADC/DAC control box.

Figures **??** to **??** show the process by which an image taken with the webcam was converted into a pressure reading. The software first identifies bounding rectangles for each individual digit. These are then further subdivided into 7 segments. If enough pixels in a given segment match the colour LCD segments, then the segment can be identified as activated. The software then creates a string corresponding to the activated segments, and looks up the digit in a dictionary.

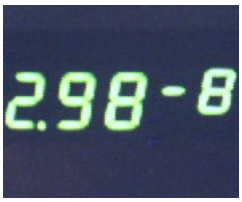

Figure 6: An unprocessed image

figures/pressure_c.jpg

Figure 7: Individual digits identified

figures/pressure_d.jpg

Figure 8: Activated segments (green) for a single digit

Appendix D - Sources of Error

GROUND LOOOOOOPS!

Appendix E - Software

No really, you don't want to know

References